

Critical state and ultimate state surface of soils: a granular solid hydrodynamic perspective

Zhichao Zhang · Xiaohui Cheng

Received: 13 August 2014 / Published online: 5 March 2015
© Springer-Verlag Berlin Heidelberg 2015

Abstract A model predicting the ultimate state surface and critical state of soils is established based on a non-equilibrium thermodynamic approach known as granular solid hydrodynamics. It offers a pressure- and density-dependent approach to assessing the elastic potential energy density of soils while taking soil cohesion into account. The ultimate state surface is quantitatively determined by the convex condition of the elastic potential energy density function with respect to the elastic strain and is compared with the state boundary surface in the critical state soil mechanics. The elastic stress is expressed by a hyper-elastic relationship. Both the critical state and the non-elastic deformation of soils depend on the evolution of elastic relaxation and granular fluctuation, which can be expressed in terms of dissipative forces and dissipative flows. The proposed model allows analysis of the soils critical state, its granular temperature and its effective stress. The predictions of triaxial compression tests of Toyoura sand and Q3 loess show that the model adequately predicts the ultimate state, the critical state and the dilation/contraction or hardening/softening of soils. Limitations of the proposed model in reproducing the density dependency of drained peak shear strength and the rate dependency of critical state are also discussed.

Keywords Critical state · Ultimate state surface · Steady state · Soil mechanics · Thermodynamics

1 Introduction

Based on a series of laboratory studies on the mechanical behavior of saturated clays, Roscoe et al. [1] proposed the well-known concept of the critical state. The critical state is a state in which the shearing deformation of soils or other granular materials continues infinitely with no changes in the effective stress and volume. In the critical state, soils are supposed to flow like frictional fluids [1]. The steady state concept was proposed for sands, according to experimental studies on their undrained triaxial shearing behavior. The steady state requires that the soil shear deformation velocity must remain constant [2]. Nevertheless, the critical state and the steady state are considered to be identical [3], and thus the critical state concept is used in this paper. The critical state is assumed to be an intrinsic property of soils. For a particular soil, all critical states fall on the same line, called the critical state line (CSL), in the space defined by effective mean pressure (p'), shear stress (q) and void ratio (e) (i.e., the $p' - q - e$ space). The CSL is commonly considered to be unique for each specific soil, irrespective of the initial state of soil.

Another important concept for modeling soil behavior is the state boundary surface (SBS). The SBS is an envelope surface of all possible states or paths in the $p' - q - e$ space. Under no conditions can any states beyond the SBS be reached. Critical state soil mechanics (CSSM) [4], based on laboratory observations, combined the classical elasto-plastic framework with the CSL and the SBS. In CSSM, the SBS is composed of a tension cutoff surface, a Roscoe surface and a Hvorslev surface (as shown in Fig. 1). Any states must, on yielding, be located on the SBS, and the CSL is considered to be the intersecting line of the Roscoe surface and the Hvorslev surface. In triaxial shear tests, the stress paths for normally consolidated (NC) soils always move along the

Z. Zhang · X. Cheng (✉)
Department of Civil Engineering, Tsinghua University,
HaiDian District, Beijing 100084, China
e-mail: chengxh@tsinghua.edu.cn

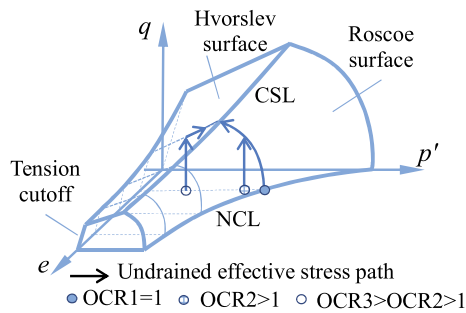


Fig. 1 Schematic diagram of the state boundary surface and the critical state line in CSSM

Roscoe surface to the critical state. The over-consolidated (OC) soils are first elastic within the SBS and then yielding after reaching the SBS, following either the Roscoe surface or the Hvorslev surface to the critical state.

The mathematical models for the SBS and the CSL have been continually developed for CSSM based on laboratory observations (Fig. 1). Such observations have been mainly in line with the linear elastic-associated hardening plasticity theory. The most popular SBS models in CSSM are the well-known Cam-Clay models [5] in both their original and simplified versions. It is worth noting that the Cam-Clay models are not rate dependent. And the Cam-Clay models are applicable only to reconstituted clays in which the true cohesion is considered to be inexistent [6]. However, some studies revealed that the true cohesion should not be neglected in reconstituted OC clays and natural clays [6–9]. For example, Shanghai Clay is a lightly overconsolidated clay with the true cohesion or bonding [10]. In fact, even for reconstituted or NC natural clays, a small cohesion may still exist due to the electrostatic attraction and the interlocking forces among soil particles [11]. Soil cohesion is preferably considered in the advanced models.

This paper proposes a new theoretical approach called granular solid hydrodynamics (GSH), which is based on non-equilibrium thermodynamics [12, 13]. In this approach, a surface bounding all accessible soil states in the $p'-q-e$ space can be naturally derived according to the elastic instability condition derived from the elastic potential energy function. In contrast to the SBS in CSSM, this surface is open in p' direction and is not directly associated with the non-elastic (or plastic) response of soil. Therefore, it is called ultimate state surface (USS), following the concept of ultimate state line in the Desai model [14], in order to distinguish it from the SBS. On the other hand, the non-elastic response of soil is described using the dissipative flow-force relationship defined in the non-equilibrium thermodynamics. This relationship is time and rate dependent and naturally allows rate dependent behavior of soil. This new approach is used to investigate the critical state of soil and USS of soil, giving a unified consideration of the possible soil cohesion.

Both the critical state and USS can be analytically derived, interpreted and modeled through this new approach to GSH, which has not received detailed discussion in previous GSH-related studies.

2 Theory based on GSH: governing equations

In the GSH approach, soils can be interpreted as transient elastic materials. As a result, the states and the unrecoverable deformation of soils can be determined by their elastic energy potential and their elastic relaxation. The following series of governing equations are thereby developed.

2.1 Effective stress formulation and elastic potential

In this paper, all stresses and strains are taken as positive under compression. For saturated soils, the total stress σ_{ij} can be expressed as the sum of the effective stress σ'_{ij} and the pore water pressure u :

$$\sigma_{ij} = \sigma'_{ij} + u\delta_{ij}, \quad (1a)$$

$$\sigma'_{ij} = \frac{\partial \omega_e}{\partial \varepsilon_{ij}^e} \quad (1b)$$

where ω_e is the elastic potential energy density and ε_{ij}^e is the elastic strain. The relation Eq. (1a) is simply the effective stress principle in soil mechanics [15]. Also, σ'_{ij} is expressed by a hyper-elastic relationship [16], as shown in Eq. (1b). The stress $\partial \omega_e / \partial \varepsilon_{ij}^e$ is called elastic stress in GSH. Other possible stresses included in σ'_{ij} (e.g., the viscous stress) are not considered here.

A formulation of ω_e for dry cohesionless granular solids was proposed by Jiang and Liu [17]. Their model is an extension of the Hertz contact model, in which the contact stiffness between solid spheres is dependent on the sphere overlap to a power of 1/2. It is proposed that, for cohesionless granular solids containing many particles, $K_e (G_e) \propto \varepsilon_v^{e\beta}$, where $K_e (G_e)$ is the secant elastic bulk (shear) modulus, $\varepsilon_v^e = \varepsilon_{kk}^e$ is the elastic volumetric strain, and β is a positive material constant.

For cohesive granular solids such as clays and silty soils, the elastic volumetric strain can be negative. Also, the shear-wave velocity and thus the elastic shear modulus G_e of saturated clays at the free stress state (i.e., $\varepsilon_{ij}^e = 0$) can be nonzero [18]. These two facts can be considered by taking $K_e (G_e) \propto (\varepsilon_v^e + c)^\beta$, where $c \geq 0$ is a cohesion-related material constant representing the maximum permissible elastic tensile volumetric strain and determining the elastic modulus of soils at free stress state. It is assumed that, this cohesion parameter can reflect the interlocking-induced cohesion as well as the true cohesion due to the cementation and electrostatic attraction among soil particles [11]. The following relationships can then be defined:

$$p' = \frac{\partial \omega_e}{\partial \varepsilon_v^e} = K_e \varepsilon_v^e + \Lambda \tag{2a}$$

$$q = \frac{\partial \omega_e}{\partial \varepsilon_s^e} = 2G_e \varepsilon_s^e \tag{2b}$$

where $\varepsilon_s^e = \sqrt{e_{ij}^e e_{ij}^e}$ is the second invariant of ε_{ij}^e ($e_{ij}^e = \varepsilon_{ij}^e - \varepsilon_v^e \delta_{ij}/3$), $p' = \sigma'_{kk}/3$ is the effective mean stress, and $q = \sqrt{s_{ij} s_{ij}}$ is the deviatoric effective stress ($s_{ij} = \sigma'_{ij} - p' \delta_{ij}$). It should be noted that q is coupled with ε_v^e and that $\partial p'/\partial \varepsilon_s^e = \partial q/\partial \varepsilon_v^e$ (because $\partial^2 \omega_e / \partial \varepsilon_v^e \partial \varepsilon_s^e = \partial^2 \omega_e / \partial \varepsilon_s^e \partial \varepsilon_v^e$). p' thus must be coupled with ε_s^e . This relationship is designated by the term Λ in Eq. (2a). Next, we define

$$K_e = B(\varepsilon_v^e + c)^\beta \tag{3a}$$

$$G_e = B\xi(\varepsilon_v^e + c)^\beta \tag{3b}$$

$$B = B_0 \exp(B_1 \rho_d) \tag{3c}$$

where B is a density dependent variable with the same dimension as the stresses, and ξ (the ratio of G_e to K_e) is considered to be constant. In Eq. (3c), B is defined as a function of the dry density of soil (ρ_d), in which B_0 and B_1 are two material constants. Equation (3c) is defined based on experimental observations of the relationship between p' and ρ_d at the critical state (see Sect. 3.2). Obviously, K_e and G_e of clays at the free stress state increase with the dry density increased. This is consistent with the conclusion reached by Mainsant et al. [18], i.e. the shear-wave velocity of saturated clays at the free stress state decays with the water content increased.

Then, from the condition $\partial p'/\partial \varepsilon_s^e = \partial q/\partial \varepsilon_v^e$, we arrive at

$$\Lambda = B\xi(\varepsilon_v^e + c)^{\beta-1} \varepsilon_s^{e2} \tag{4}$$

Therefore, we can obtain the following formulation of ω_e from Eqs. (2, 3):

$$\omega_e = B(\varepsilon_v^e + c)^\beta \left[\frac{\varepsilon_v^{e2}}{\beta + 2} + \frac{c\beta \varepsilon_v^e - c^2}{(\beta + 1)(\beta + 2)} + \xi \varepsilon_s^{e2} \right] + \frac{Bc^{\beta+2}}{(\beta + 1)(\beta + 2)} \tag{5a}$$

When taking $c = 0$, Eq. (5a) is reduced to the model for cohesionless granular solids [17]:

$$\omega_e = B\varepsilon_v^{e\beta} \left(\frac{1}{\beta + 2} \varepsilon_v^{e2} + \xi \varepsilon_s^{e2} \right) \tag{5b}$$

2.2 Elastic relaxation and granular fluctuation

Under external loadings, soils tend to exhibit unrecoverable deformation due to elastic relaxation, which is an important feature of transient elastic materials. Accordingly, we divide the total strain of soil ε_{ij} into the elastic strain and the non-elastic strain ε_{ij}^D , i.e., $\varepsilon_{ij} = \varepsilon_{ij}^e + \varepsilon_{ij}^D$. In GSH, ε_{ij}^D evolves

only when the so-called granular fluctuation is stimulated. Moreover, the non-elastic strain rate is simply the dissipative flow of the elastic relaxation with a dissipative force of $\partial \omega_e / \partial \varepsilon_{ij}^e$. In that case, the granular fluctuation represents the random disordered deviation between the movements of individual particles of granular solids and their macro average movements. In other words, this fluctuation implies relative movements between soil particles such as sliding, collisions and rotations, all of which are important sources of the unrecoverable deformation.

Following the concept of entropy, the concept of granular entropy was proposed in GSH to describe the severe degrees of granular fluctuation. Similar concepts have also been introduced by other researchers [19,20]. Based on non-equilibrium thermodynamics and the relaxation time concept, the following evolution law for ε_{ij}^D has been proposed [13]:

$$d_t \varepsilon_{ij}^D = \lambda_s T_g^a e_{ij}^e + \lambda_v T_g^a \varepsilon_v^e \delta_{ij} \tag{6}$$

where d_t is the material derivative operator; λ_s and λ_v are migration coefficients; a is a material constant, and T_g (called the granular temperature) is the conjugate variable of the granular entropy. The granular fluctuation can be excited by “shear and compressional flows” of the soil skeleton [13] so that the strain rate is used as a driving force of the granular fluctuation. In addition, the granular fluctuation displays a characteristic of relaxation, which means that once triggered, the granular fluctuation can be attenuated into the macro dissipation over time due to the non-elastic inter-particle contacts. In other words, a conversion from the granular entropy to the (real) entropy should be considered. Thus, according to GSH, the granular entropy should obey a balanced equation similar to the equation for the entropy:

$$\rho_d d_t v_g = \frac{\eta_g T_g v_{ij}^* v_{ij}^* + \zeta_g T_g v_v^2}{T_g} - \gamma T_g \tag{7a}$$

$$v_g = b T_g \tag{7b}$$

where v_g is the specific granular entropy; b is a material constant; $v_v = d_t \varepsilon_{kk}$ is the volumetric strain rate, and $v_{ij}^* = d_t(\varepsilon_{ij} - \varepsilon_{kk} \delta_{ij}/3)$ is the deviatoric (or shear) strain rate. η_g (ζ_g) is the migration coefficient for the granular fluctuation excited by the shear deformation (compressional deformation), and γ is the migration coefficient for the relaxation of granular fluctuation.

3 Critical state and ultimate state surface based on GSH

Based on the governing equations developed above, the theoretical expressions for the critical state and USS of saturated

soils are given in this section, and the comparisons between the GSH approach and the classical CSSM approach are discussed.

3.1 Ultimate state surface (USS)

As the effective stresses of soils can be approximated by the elastic stresses derived from the GSH approach, the USS that bounds all accessible states of a soil can be given by the elastic stability condition, which requires that ω_e be a convex function of the elastic strain. This convex condition of ω_e is equivalent to the positive definiteness condition of the Hessian matrix $[H_{ij}] = \partial^2\omega_e/(\partial X_i\partial X_j)$ ($i, j = 1, 2$; $X_1 = \varepsilon_v^e, X_2 = \varepsilon_s^e$), which is also the tangential elastic stiffness matrix. This condition can be further determined by the positive conditions of all of the leading principal minors of $[H_{ij}]$, in which the following condition can be used to find the USS of soils in the $p - q - \rho_d$ space:

$$\frac{\partial^2\omega_e}{\partial\varepsilon_v^e\partial\varepsilon_v^e} \frac{\partial^2\omega_e}{\partial\varepsilon_s^e\partial\varepsilon_s^e} - \left(\frac{\partial^2\omega_e}{\partial\varepsilon_v^e\partial\varepsilon_s^e}\right)^2 > 0 \tag{8}$$

Substituting Eq. (5a) into Eq. (8) results in

$$(\varepsilon_v^e + c)[(\beta + 1)\varepsilon_v^e + c] > 2\beta(\beta + 1)\xi\varepsilon_s^e{}^2 \tag{9}$$

Equating the left and right sides of the inequality Eq. (9), an elastic stability line (ESL) in the $\varepsilon_v^e - \varepsilon_s^e$ space can be determined. According to Eqs. (2, 3, 5), for a given ρ_d , all values ε_v^e and ε_s^e on the ESL form a ultimate state line (USL) in the $p' - q$ space. All USLs corresponding to different ρ_d therefore form an USS in the $p' - q - e$ space (void ratio $e = G_s/\rho_d - 1$, where G_s is the intrinsic density of the soil particles). Apparently, the USS based on the GSH approach corresponds to the states at which the tangential elastic stiffness matrix becomes singular and the convex condition of ω_e with respect to the elastic strain is initially violated. For any elastic strain variation $X = [\delta\varepsilon_v^e, \delta\varepsilon_s^e]$ (δ being the variation operator), this convexity implies that $X[H_{ij}]X^T = \delta\pi_{ij}\delta\varepsilon_{ij}^e > 0$. The ultimate state thus also corresponds to the violation of the positive condition of the work done by the effective stress variation on the induced elastic strain variation.

Figure 2 shows an example of the USL for a given ρ_d . Taking $\varepsilon_s^e = 0$ in Eq. (9), the intercept of the USL on the p' axis (which can be referred to as the tensile strength of the soil) is derived as follows:

$$p'_t = B(\varepsilon_{vt}^e + c)^\beta \varepsilon_{vt}^e, \quad \varepsilon_{vt}^e = \max \left\{ -c, -\frac{c}{\beta + 1} \right\} \tag{10}$$

Apparently, the parameter c controls the cohesion of soils. As in Fig. 2, a larger c leads to a larger allowable tensile effective

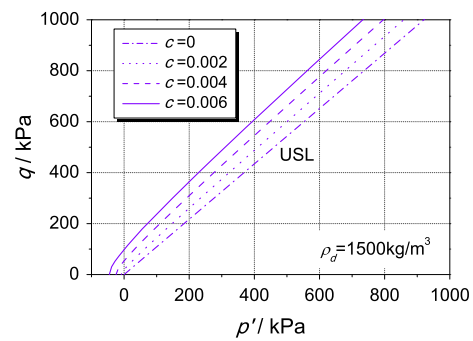


Fig. 2 Ultimate state line (USL) for various c values

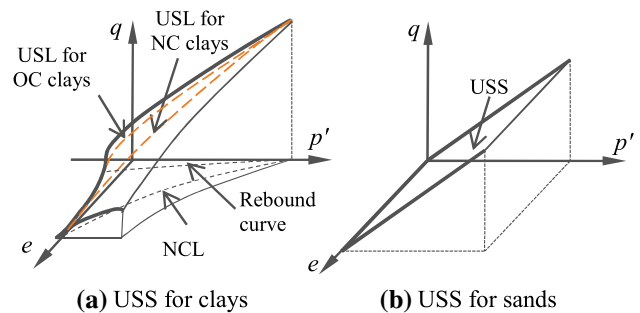


Fig. 3 Schematic diagram of the ultimate state surface as defined in this paper

stress region. When $c = 0$, states in the tensile region are impossible, which is just the situation found in sands. The ESLs for $c \neq 0$ are non-linear, but those for $c = 0$ are linear. As a result, the USS in the $p' - q - e$ space for clays is a curved surface, but for sands it is a plane surface, as shown in Fig. 3. Moreover, the projection of the USS for clays on the $p' - q$ plane is a surface, and the projection for sands is a line. From Eqs. (3) and (10), the cohesion is dependent on the dry density and the stress history. The USL for NC clays with low dry densities is a line approximately passing through the original point (i.e., p'_t is very small but nonzero), while the USL for OC clays possesses a much larger p'_t due to their higher dry densities (the USLs for NC or OC clays are the intersecting lines of the USS and the surface that is parallel to the q axis and passes through the NCL or the rebound curve, see Fig. 3a). This OCR dependency of the cohesion for clays is consistent with the conclusions reported by literatures [7–9, 11].

Outside the USS, soils are mechanically unstable [13], and therefore soils cannot reach states beyond the USS. Having noted that p' and q can be determined if the elastic strain invariants and the dry density are given, we can examine the USS represented by p' and q by following any arbitrarily selected evolution paths of $\varepsilon_v^e, \varepsilon_s^e$ and ρ_d . In Figs. 4 and 5, two types of path in the $p' - q - \rho_d$ space are examined: (1) the constant volume (or constant ρ_d) shear test, as shown in Fig. 4, and (2) the triaxial compression test in which

Fig. 4 The $p - q$ paths (right) under the assumed loading paths in the $\varepsilon_v^e - \varepsilon_s^e$ space (left) with a constant dry density

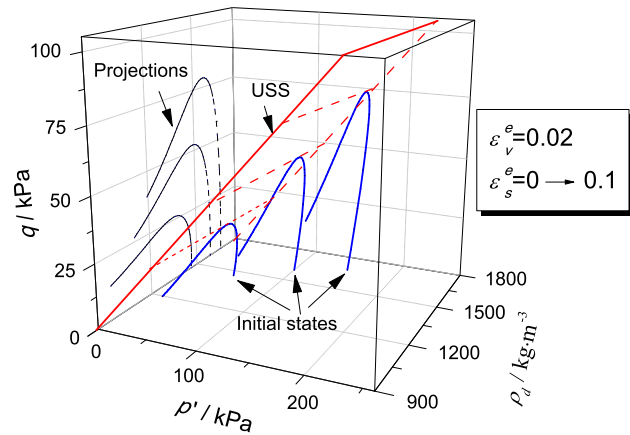
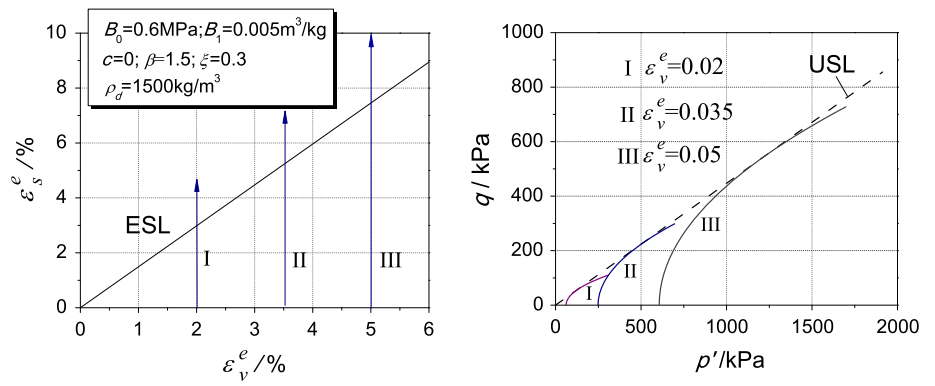


Fig. 5 Triaxial shear paths ($\Delta p' = \Delta q/3$) in the $p - q - \rho_d$ space (parameters used are the same as those shown in Fig. 4; $\varepsilon_v^e = 0.02$, and ε_s^e varies from 0 to 0.1)

$\Delta q / \Delta p' = 3$ (Δ is the increment sign), as shown in Fig. 5. In both cases, ε_v^e is first fixed arbitrarily, and then ε_s^e is increased continuously. In the case (2), ρ_d is calculated according to Eqs. (2b and 3c) as a function of q , ε_v^e and ε_s^e . The results show that the $p' - q - \rho_d$ paths become tangent to the USS (or USL) when the $\varepsilon_s^e - \varepsilon_v^e$ paths reach the ESL. However, these paths never cross the USS under any condition, even if the elastic stability condition (Eq. 9) is violated.

3.2 Critical states

3.2.1 Definition and analytical expressions

From Eq. (6) and the relation $\varepsilon_{ij} = \varepsilon_{ij}^e + \varepsilon_{ij}^D$, the elastic strain rates can be written in terms of the elastic strain invariants and total strain rates as follows:

$$d_t \varepsilon_v^e = v_v - 3\lambda_v T_g^a \varepsilon_v^e \quad (11a)$$

$$d_t \varepsilon_s^e = \frac{e_{ij}^e}{\varepsilon_s^e} (v_{ij}^* - \lambda_s T_g^a e_{ij}^e) \quad (11b)$$

For the critical states, the soil volume and the effective stress should be kept constant, and the deviatoric (shear) strain

rate $v_{ij}^* \neq 0$. Therefore, according to Eqs. (2, 3), the elastic strain invariants must be constant at the critical state. Noting Eqs. (7) and (11), this condition further requires a constant v_{ij}^* at the critical state. In fact, it can be found that $v_v = 0$ and $v_{ij}^* = \text{constant}$ are the two necessary and sufficient conditions for deciding whether the critical state can be reached. If these two conditions can be satisfied, soils will be sheared at a constant deviatoric strain rate without any changes in the granular temperature T_g , the dry density ρ_d and the elastic strain invariants (ε_v^e and ε_s^e). This state is then referred to as the critical state defined in this paper. As discussed above, the critical state cannot be reached if the total strain rate is varying. Therefore, the condition of shearing at a constant strain rate (or at “constant velocity of deformation”, as proposed for the steady state [2]) is one of necessities for the critical state based on the GSH approach.

The critical state can also be interpreted as a state in which the following special situations of energy dissipations apply: (1) the granular fluctuation excited by shear deformation balances the relaxation of granular fluctuation, i.e., $\rho_d d_t v_g = 0$ (see Eq. 7); (2) all of the input mechanical energy is dissipated by the elastic relaxation, and no more elastic potential is stored, i.e., $d_t \varepsilon_{ij} = d_t \varepsilon_{ij}^D$ or $d_t \varepsilon_{ij}^e = 0$. Thus, from Eqs. (2, 7, 11), one can derive the following expressions for soils at the critical state:

$$(T_g)_{cr} = \frac{\eta_g v_{ij}^* v_{ij}^*}{\gamma} \quad (12a)$$

$$(\lambda_v \varepsilon_v^e)_{cr} = 0 \quad (12b)$$

$$(\varepsilon_s^e)_{cr} = \lambda_s^{-1} \left(\frac{\gamma}{\eta_g} \right)^{2a} (v_{ij}^* v_{ij}^*)^{1-2a} \quad (12c)$$

$$p'_{cr} = B_0 \exp[B_1(\rho_d)_{cr}] [(\varepsilon_v^e)_{cr} + c]^{\beta-1} \cdot [(\varepsilon_v^e)_{cr}^2 + c(\varepsilon_v^e)_{cr} + \xi(\varepsilon_s^e)_{cr}^2] \quad (12d)$$

$$q_{cr} = 2B_0 \exp[B_1(\rho_d)_{cr}] [(\varepsilon_v^e)_{cr} + c]^{\beta} \xi (\varepsilon_s^e)_{cr} \quad (12e)$$

where symbols with the subscript “cr” represent the corresponding values at the critical state.

According to Eqs. (12d, 12e), the critical states are located on a linear CSL (critical state line) in the $\ln p'_{cr} - \ln q_{cr} -$

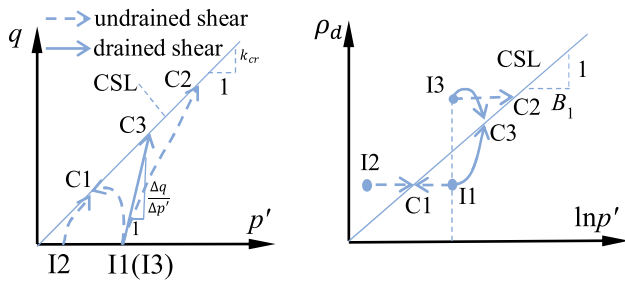


Fig. 6 Schematic diagram of the critical state line (CSL) (“I” represents the initial-state point and “C” represents the critical state point)

$(\rho_d)_{cr}$ space, as q_{cr}/p'_{cr} is constant and $(\partial \ln p'_{cr})/(\partial (\rho_d)_{cr}) = B_1$, as shown in Fig. 6. This conclusion can be validated by many experimental studies of the CSL [3, 21, 22].

It should be noted that if the migration coefficient λ_v is taken as a constant, then the elastic volumetric strain at the critical state has to vanish according to Eq. (12b). If so, i.e., $(\varepsilon_v^e)_{cr} = 0$, then the critical shear strength q_{cr} will always be zero for soils without cohesion (in which $c = 0$) (see Eq. 12e). However, many experimental studies show nonzero q_{cr} for sands [3], and the level of q_{cr} depends on the density of sand. To deal with this problem, the migration coefficient λ_v should be a state-dependent variable, and $(\lambda_v)_{cr} = 0$ at the critical state. The λ_v can be modeled according to the experimental observation that the critical state is usually close to the USS [2, 3, 5, 23, 24]. In fact, there are also laboratory data showing critical states that are far away from the USS [25]. The underlying mechanism for this difference is not yet clear. However, from the point view of modeling, the relation between the critical state and the USS can be simply defined through a positive dimensionless parameter ψ . When $\psi = 1$, the critical state is exactly located on the USS. Accordingly, noting the condition Eq. (9), λ_v can be defined as

$$\begin{cases} \lambda_v = \lambda_{v0} \left(1 - \psi \sqrt{\frac{\beta(\beta+1)\xi(\varepsilon_s^e)^2}{(\varepsilon_v^e+c)[(\beta+1)\varepsilon_v^e+c]}} \right) \\ \lambda_v \geq -\frac{\lambda_s e_{ij}^e s_{ij}}{3\varepsilon_v^e p'} \end{cases} \quad (13)$$

where λ_{v0} is a material constant. Apparently, taking $\psi \neq 1$ results in critical states that are beneath the USS. The energy dissipation rate $R = \sigma'_{ij} d_t \varepsilon_{ij}^D = T_g^a (3\lambda_v \varepsilon_v^e p' + \lambda_s e_{ij}^e s_{ij})$. Noting that λ_v will become negative for the states beyond the CSL, $\lambda_v \geq -\lambda_s e_{ij}^e s_{ij} / (3\varepsilon_v^e p')$ is required in Eq. (13) to ensure $R \geq 0$.

3.2.2 Rate and initial-state dependency

One of the features of the critical state as described in this paper is the strain-rate dependency. As shown in Eq. (12c, 12e), the critical shear strength may vary with the strain rate,

depending on the value of the parameter a . Some experimental studies [23] show that clays usually have larger critical shear strengths under larger shear strain rates. Such results imply that $a < 0.5$ for clays ($a = 0.455$ is assumed in this paper). However, the mechanical behavior of sands is usually considered to be strain-rate independent [3], which requires $1 - 2a = 0$ (i.e., $a = 0.5$) in the proposed model. Meanwhile, according to Eqs. (12d, 12e), the critical state friction angle represented by the slope of CSL $k_{cr} = q_{cr}/q'_{cr}$ is also dependent on the strain rate. However, it is more likely that k_{cr} is a constant independent on the strain rate [26]. In order to represent this feature by the model, Eq. (13) should be redefined as

$$\begin{cases} \lambda_v = \lambda_{v0} \left[1 - \sqrt{\frac{(\varepsilon_v^e+c)\xi\varepsilon_s^e}{k_{cr}[(\varepsilon_v^e)^2+c\varepsilon_v^e+\xi(\varepsilon_s^e)^2]}} \right] \\ \lambda_v \geq -\frac{\lambda_s e_{ij}^e s_{ij}}{3\varepsilon_v^e p'} \end{cases} \quad (14)$$

Equation (14) can also be interpreted as that the parameter ψ in Eq. (13) is no longer a constant. But in the following analysis, Eq. (13) with constant ψ was used, as the strain rate dependency of mechanical behavior of soils is out of focus of the present study.

The critical state described by Eq. (12) is dependent on the initial state of the soil. Here, we consider only the rate-independent case, i.e., $a = 0.5$. The critical state in undrained shears is uniquely determined by the initial dry density (which remains constant in the undrained shears). For example, in Fig. 6, the initial-state points I1 and I2, which have the same density but different confining pressures, correspond to the same undrained critical state (C1). Meanwhile, the initial points I1 and I3, which have the same initial confining pressure, correspond to different undrained critical states (C1 and C2). For drained shears, we define a constant stress increment ratio $\Delta q/\Delta p'$. (For triaxial drained shears, $\Delta q/\Delta p' = 3$.) Then, the drained critical states in the $p' - q$ space are uniquely determined by the initial confining pressure. As in Fig. 6, the initial points I1 and I3 (although they have different initial dry densities) correspond to the same drained critical state (C3). However, the volumetric deformation from the initial state to the critical state is primarily dependent on the initial dry density $(\rho_d)_0$. The soil undergoes a contraction when $(\rho_d)_0 < (\rho_d)_{cr}$ (I1–C3 in Fig. 6 (right)) and undergoes a dilation when $(\rho_d)_0 > (\rho_d)_{cr}$ (I3–C3 in Fig. 6 (right)). Using the GSH approach, the initial-state dependency discussed above can be accurately predicted. The predictions regarding this issue are presented in Sect. 4.1.

3.2.3 Drainage conditions

In the above discussions, $v_v = 0$ and $v_{ij}^* = \text{constant}$ are taken as two basic requirements for the critical state to be attained.

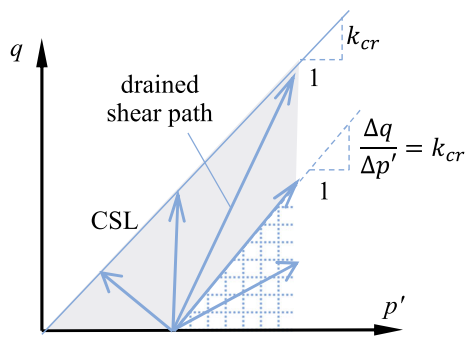


Fig. 7 Drained shear paths in the $p' - q$ space

However, the state of shearing without any change in the soil volume cannot always be reached, as this state depends on the drainage condition and the stress path. For undrained shear loadings, $v_v = 0$ is naturally satisfied, and thus the critical state can always be reached if the shear strain rate is controlled to be constant. For drained shears, whether $v_v = 0$ can be eventually reached depends on the stress increment ratio $\Delta q/\Delta p'$. We denote the slope of CSL in the $p' - q$ space as $k_{cr} = q_{cr}/p'_{cr}$. As shown in Fig. 7, provided that the shear strain rate is kept constant, the critical state can be reached when $\Delta q/\Delta p' > k_{cr}$ or $\Delta q/\Delta p' < 0$. In that case, the soil volume will eventually stop changing. However, when $0 \leq \Delta q/\Delta p' \leq k_{cr}$, the critical state can never be reached, and the soil volume will develop continuously. This stress-path dependent feature of the critical state is validated in the simulation results given in Sect. 4.1. To sum up, the necessary and sufficient conditions under which the critical state can be reached are as follows:

$$\begin{cases} v_{ij}^* = \text{constant} \\ \frac{\Delta q}{\Delta p'} \in [-\infty, 0) \cup (k_{cr}, +\infty] \end{cases} \quad (\text{drained shear}) \quad (15)$$

$$v_{ij}^* = \text{constant} \quad (\text{undrained shear})$$

3.3 Comparisons between GSH and classical CSSM

The main differences between GSH and classical CSSM include the following:

1. The definition of critical state as used in this paper involves more state variables and energy processes than the definition used in classical CSSM. The critical state described in this paper depends on the evolutions of granular fluctuation and elastic relaxation. Both of these factors are described by the concepts of dissipative force and dissipative flow, which lead to a time- and rate-dependent model. As a result, the critical state can only be reached at a constant shearing rate. However, the critical state in

the classical CSSM is based on the associated plastic flow rule in the elasto-plastic framework and is therefore time and rate independent.

2. In CSSM, the plastic deformation is determined by the flow rule depending on the plastic potential surface which is also the SBS when associated flow rule is assumed. However, in this study there is no surface that is directly associated with the plastic soil deformation. Instead, the responses of the soil are completely calculated by the evolutions of energy storage (elastic potential) and energy dissipations (elastic relaxation and granular fluctuation). Correspondingly, the concept of yield surface or plastic potential surface is not used in this study.
3. Even without the concept of SBS, the present model is capable of predicting the fundamental behavior of soils such as the ultimate state, the critical state and also the asymptotic state. The asymptotic state is defined as the state reached after a sufficiently long proportional stretching with a constant direction of the strain rate [27]. The analytical expressions for the asymptotic state can be derived using the same method for the critical state presented in Sect. 3.2.1, simply by introducing the strain-controlled loading conditions (e.g., $v_a = \text{constant}$ and $v_v/v_a = \text{constant}$ for the axisymmetric stress and strain states, where v_a is the axial strain rate). Therefore, the critical state is a special asymptotic state at which $v_v = 0$. Figure 8 gives some simulation results of asymptotic states reached under three different strain rate paths: confined compression (curves A), undrained shearing (curves B), and rebounding expansion (curves C). For all the three paths, the asymptotic states at which $p'/q = \text{constant}$ and $\ln p' \propto \ln(1 + e)$ are finally reached.

4 Model predictions for sand and clay

Based on the theory described above, the critical state and the ultimate state of Toyoura sand [28] and Q3 loess [29] under triaxial conditions are predicted in this section. Under triaxial conditions, the stress and strain tensors are diagonal, with $\sigma_1 = \sigma_{11}$, $\sigma_2 = \sigma_{22}$, $\sigma_3 = \sigma_{33}$, $\varepsilon_1 = \varepsilon_{11}$, $\varepsilon_2 = \varepsilon_{22}$ and $\varepsilon_3 = \varepsilon_{33}$, where the subscript 1 represents the axial direction. In triaxial compression tests, $\sigma_2 = \sigma_3$, $\varepsilon_2 = \varepsilon_3$ and $\Delta q/\Delta p = 3$, where

$$q = \sigma_1 - \sigma_3, \quad p = \frac{\sigma_1 + 2\sigma_3}{3} = p' + u \quad (16)$$

The σ_3 and the axial strain rate ($d_t \varepsilon_1$) are usually controlled to be constant in tests. Under drained conditions, $u = 0$, and $d_t \varepsilon_v = d_t(\varepsilon_1 + 2\varepsilon_3)/3 = 0$. Then, using Eqs. (2, 3, 5–7 and 11), the triaxial responses of soils can be calculated. The needed parameters are listed in Tables 1

Fig. 8 Simulation results of asymptotic states using the model in this study (σ_a and σ_r are the axial and radial stresses, respectively; the initial states are arbitrarily selected; parameters used: $B_0 = 10$ kPa, $B_1 = 0.0075$ m³/kg, $\xi = 0.59$, $\beta = 1.5$, $c = 0$, $\lambda_{v0}/\lambda_s = 0.2$, $\gamma/b = 5000$ kg/m³/min, $(\lambda_s)^{1/a}\eta_g/b = 7.5 \times 10^7$ kg/m³/min and $\zeta_g/\eta_g = 0.5$)

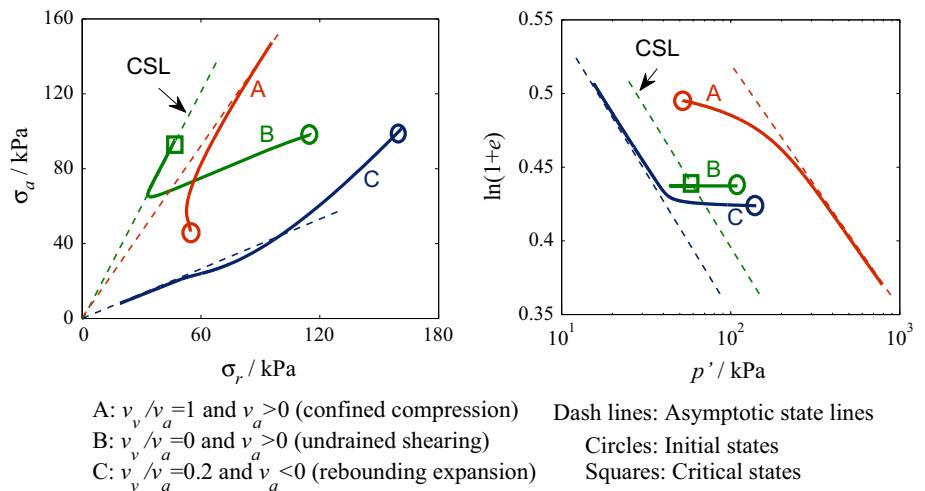


Table 1 Model parameters for Toyoura sand

$B_0 = 1$ Pa; $B_1 = 0.0129$ m ³ /kg; $\xi = 0.59$ $\beta = 0.5$
$c = 0$; $\lambda_{v0}/\lambda_s = 0.167$; $\gamma/b = 5000$ kg/m ³ /min
$(\lambda_s)^{1/a}\eta_g/b = 2.62 \times 10^6$ kg/m ³ /min
$\zeta_g/\eta_g = 2$; $\psi = 1.5$; $a = 0.5$

Table 2 Model parameters for Q3 loess

$B_0 = 14.8$ Pa; $B_1 = 0.0094$ m ³ /kg; $\xi = 0.33$ $\beta = 1.5$
$c = 0.0462$; $\lambda_{v0}/\lambda_s = 0.15$; $\gamma/b = 1500$ kg/m ³ /min
$(\lambda_s)^{1/a}\eta_g/b = 8.66 \times 10^4$ kg/m ³ /min
$\zeta_g/\eta_g = 1$; $\psi = 1$; $a = 0.455$

or 2. It should be noted that determining four relative values between the six migration coefficients (λ_{v0} , λ_s , η_g , ζ_g , γ and b) is sufficient to solve the equations. The parameters can be calibrated according to conventional laboratory tests such as the isotropic compression and undrained (or drained) triaxial compression tests. Once this calibration is done, more tests can be predicted using the calibrated parameters. The parameters used in this paper for Toyoura sand and Q3 loess are listed in Tables 1 and 2, respectively.

4.1 Predictions for Toyoura sand

Figures 9 and 10 show the simulation results of undrained and drained triaxial compression tests for Toyoura sand [28]. Only the test with an initial void ratio of $e_0 = 0.753$ and an initial confine pressure of $p'_0 = 1000$ kPa is used in the parameter determination. Thus, in Figs. 9 and 10, all other tests are predicted using the same parameters (the axial strain rate is 5%/min in the predictions). The predicted results are fairly consistent with the measured results. Under undrained

conditions, the sand samples with the same ρ_d reach the same critical state even if they are under a different p'_0 . However, the undrained responses before the critical state are significantly affected by p'_0 . Under the same e_0 , a smaller p'_0 results in a stronger dilatancy, a smaller shear modulus and a larger axial strain under which the critical state is reached. As shown in Fig. 10, the same critical state is reached for drained sand samples under the same p'_0 , irrespective of the initial ρ_d . In that case, contraction and dilation are observed for samples with an initial ρ_d lower or higher than the critical ρ_d , respectively. The mechanism of the initial-state dependency predicted above has been given in Fig. 6.

Furthermore, noting that ψ (see Eq. 13) is taken as 1.5 in this case, the critical state is located beneath the USS (or USL), and the ultimate state is reached only for strongly dilative samples, as shown in Figs. 9 and 10. For the drained test with $e_0 = 0.81$ (Fig. 10), a minor contraction is first observed with the strain hardening. Then a significant dilation begins after the ultimate state is reached, followed by the strain softening. In comparing the three stress–strain curves in Fig. 10, it is clearly more difficult for the soil samples with relatively heavy dilatancy ($e_0 = 0.81$) or heavy contraction ($e_0 = 0.96$) to reach the critical state. Moreover, a larger initial dry density (or a smaller initial void ratio) results in a larger drained peak shear strength (as shown in Fig. 10). During the drained triaxial compression tests of sands the USL in the $q - \rho_d$ space under a particular p'_0 is in parallel with the ρ_d -axis so that the dependency of drained peak shear strength on dry density disappear when the critical state is located on the USL (i.e. $\psi = 1$). This is a limitation of the present model, which needs to be improved in the future research.

As predicted above, the critical state can be reached under drained triaxial shearing. However, as discussed in the Sect. 3.2.3, the critical state cannot always be reached under every drained shear loading. Under drained condi-

Fig. 9 Prediction of undrained triaxial compression tests of Toyoura sand

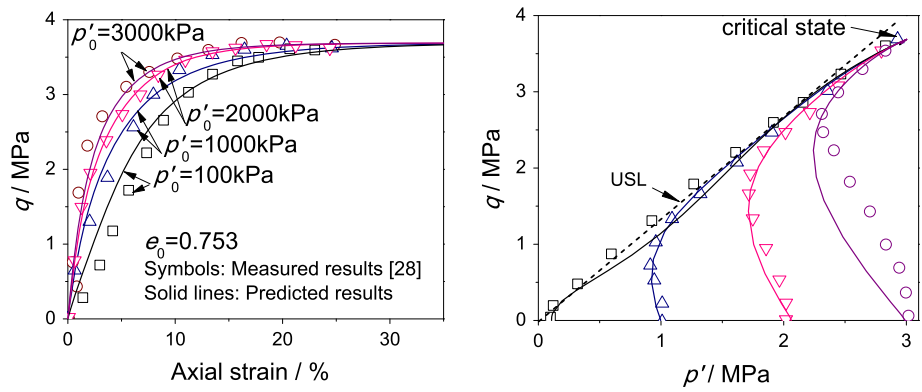


Fig. 10 Prediction of drained triaxial compression tests of Toyoura sand ($\rho_d = G_s/(1 + e)$ and $G_s = 2700 \text{ kg/m}^3$)

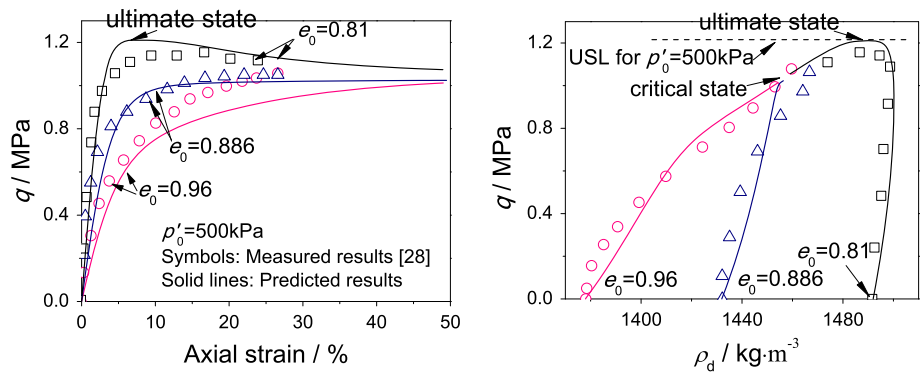
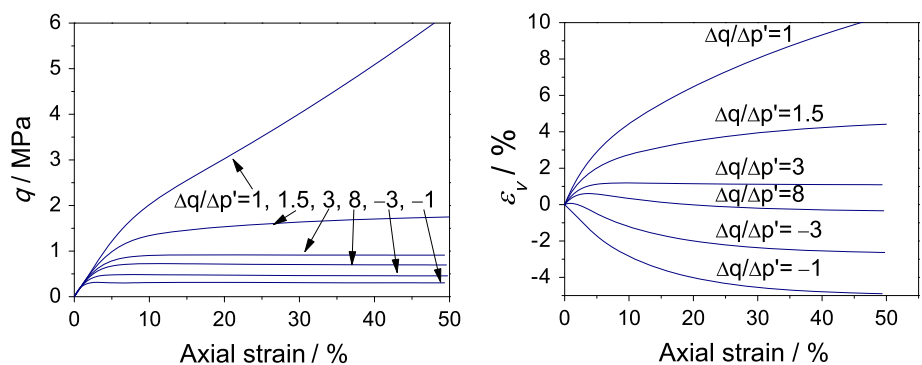


Fig. 11 Effect of shear path on the drained shearing responses of Toyoura sand ($p'_0 = 500 \text{ kPa}$ and $e_0 = 0.886$)

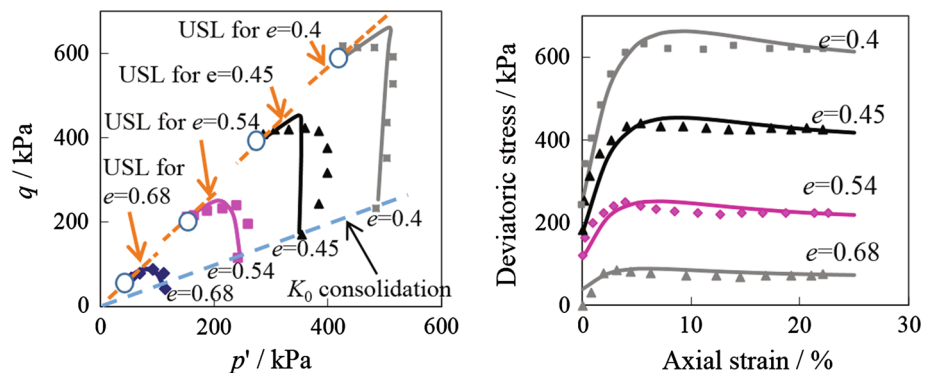


tions, the critical state can be observed only when the stress increment ratio, $\Delta q/\Delta p'$, meets the condition shown in Eq. (15) (from Fig. 9, the k_{cr} for Toyoura sand is about 1.27). Figure 11 shows the simulation results of the drained shear responses under six different values of $\Delta q/\Delta p'$. Obviously, when $0 < \Delta q/\Delta p' < 1.27$, the volumetric strain is continuously increased without reaching the critical state at which $d_t \epsilon_v = 0$ is required. The same conclusion can be drawn for the deviatoric stress q . However, when $\Delta q/\Delta p' > 1.27$ or $\Delta q/\Delta p' < 0$, the critical state can always be reached. Moreover, a larger positive $\Delta q/\Delta p'$ or a larger negative $\Delta q/\Delta p'$ results in a more significant dilation.

4.2 Predictions for Q3 loess

Figure 12 shows the prediction results of the undrained triaxial compression tests for Q3 loess [29], in which the test with $e = 0.54$ is used to determine the model parameters. The loess samples are first K_0 -consolidated to different non-isotropic stress states and then triaxially sheared under undrained conditions. The prediction results are also in agreement with the measured data. Taking $\psi = 1$ for the loess (see Table 2), the critical states predicted are always located on the USS, and the $p' - q$ paths become tangent to the USL for the corresponding void ratio e . It should be noted that unlike the USLs for sands, the USLs for the different given e (or

Fig. 12 Prediction of undrained triaxial compression tests of Q3 loess ($G_s = 2750 \text{ kg/m}^3$; the dots are measured data from [29]; the circular symbols represent the critical states)



ρ_d) of clays do not coincide with each other. However, the critical states for different e values fall on the same CSL in the $p' - q$ space.

5 Concluding remarks

A model predicting the ultimate state surface (USS) and critical state has been established for saturated soils based on the GSH approach. This approach differs from that used in classical critical state soil mechanics (CSSM). This new approach improves understanding of the USS and the critical state from the perspective of thermodynamics. The GSH approach also predicts the mechanical behavior of soils more accurately. The main contributions of this paper include the following:

1. A model is proposed that assesses the elastic potential of soil and takes the degree of soil cohesion into account. It is shown that the USS of soil corresponds to the convexity of the elastic potential energy density function with respect to the elastic strain. Using this model, a curved USS for clays and a plane USS for sands in the $p' - q - \rho_d$ space are determined quantitatively.
2. Granular soil deformation is controlled by elastic relaxation and granular fluctuation, which are thermodynamically defined as time- and rate-dependent functions of the elastic strain and the granular temperature. The critical state of soils is analytically formulated based on this approach. This analysis reveals that the critical state of soils is dependent on the initial state, rate and drainage conditions. A clear and analytical explanation of this important concept is given.
3. Without the concepts such as SBS (or the yield surface) and the plastic potential that are needed in the classical CSSM, the proposed model based on the extended GSH can also predict the fundamental behavior of soils, such as the ultimate state, the critical state and the asymptotic state. However, the density dependency of drained peak shear strength for sands cannot be appropriately predicted when taking the parameter $\psi = 1$. Meanwhile, the rate

independency of the slope of CSL is not considered in the simulations made in this study. Both deficiencies of the present model need to be improved in the future study.

Acknowledgments This study was supported by the Tsing-hua-Cambridge-MIT low carbon energy university alliance (TCM-LCEUA) seed funding project, to which we hereby express our sincere gratitude.

Conflict of interest This study is finically supported by the Tsinghua-Cambridge-MIT Low Carbon Energy University Alliance (LCEUA) seed funding project. The funders had no role in study design, data collection and analysis, decision to publish, or preparation of the manuscript. All the data presented in this study have not been published anywhere else. Also, we declare that there is no conflict of interests regarding this manuscript. None of the authors have any financial and personal relationships with other people or organizations that can inappropriately influence the quality of the work presented in this manuscript. There is no professional or other personal interest of any nature or kind in any product, service and/or company that could be construed as influencing the position presented in, or the review of, this manuscript. Opinions or points of view expressed are those of the authors and do not necessarily reflect the official position or policies of the LCEUA.

References

1. Roscoe, K.H., Schofield, A.N., Wroth, C.P.: On the yielding of soils. *Geotechnique* **8**(1), 22–53 (1958)
2. Poulos, S.J.: The steady state of deformation. *J. Geotech. Eng. ASCE* **107**(5), 553–562 (1981)
3. Been, K., Jefferies, M.G., Hachey, J.: The critical state of sands. *Geotechnique* **41**(3), 365–381 (1991)
4. Poulos, S.J., Castro, G., France, J.W.: Liquefaction evaluation procedure. *J. Geotech. Eng. Am. Soc. Civ. Eng.* **111**(6), 772–792 (1985)
5. Roscoe, K.H., Burland, J.B.: On the generalised stress–strain behaviour of ‘wet’ clay. In: Heyman, J., Leckie, F.A. (eds.) *Engineering Plasticity*, pp. 535–609. Cambridge University Press, Cambridge (1968)
6. Yan, W.M., Li, X.S.: A model for natural soil with bonds. *Geotechnique* **61**(2), 96–106 (2011)
7. Briaud, J.L.: *Geotechnical engineering: unsaturated and saturated soils*. Wiley, Hoboken (2013)
8. Skempton, A.W.: The colloidal ‘activity’ of clays. In: Skempton, A.W. (ed.) *Selected Papers on Soil Mechanics*, pp. 106–118. Thomas Telford Ltd., London (1984)

9. Skempton, A.W., Bishop, A.W.: The measurement of the shear strength of soils. *Geotechnique* **2**(2), 90–108 (1950)
10. Li, Q., NG, C.W.W., Liu, G.B.: Low secondary compressibility and shear strength of Shanghai Clay. *J. Cent. South Univ.* **19**, 2323–2332 (2012)
11. Mitchell, J.K.: *Fundamentals of Soil Behavior*. Wiley, Berkeley (1993)
12. Jiang, Y.M., Liu, M.: From elasticity to hypoplasticity: dynamics of granular solids. *Phys. Rev. Lett.* **99**, 105501 (2007)
13. Jiang, Y.M., Liu, M.: Granular solid hydrodynamics. *Granul. Matter* **11**(3), 139–156 (2009)
14. Liu, X., Cheng, X.H., Scarpas, A., et al.: Numerical modeling of nonlinear response of soil. Part 1: constitutive model. *Int. J. Solids Struct.* **42**, 1849–1881 (2005)
15. Bishop, A.W.: The principle of effective stress. *Tek. Ukebl.* **39**, 859–863 (1959)
16. Houlby, G.T., Amorosi, A., Rojas, E.: Elastic moduli of soils dependent on pressure: a hyperelastic formulation. *Geotechnique* **55**(5), 383–392 (2005)
17. Jiang, Y.M., Liu, M.: Granular elasticity without the coulomb condition. *Phys. Rev. Lett.* **91**, 144301 (2003)
18. Mainsant, G., Jongmans, D., Chambon, G., et al.: Shear-wave velocity as an indicator for rheological changes in clay materials: Lessons from laboratory experiments. *Geophys. Res. Lett.* **39**, L19301 (2012)
19. Haff, P.K.: Grain flow as a fluid-mechanical phenomenon. *J. Fluid Mech.* **134**, 401–430 (1983)
20. Jenkins, J.T., Savage, S.B.: A theory for the rapid flow of identical, smooth, nearly elastic particles. *J. Fluid Mech.* **130**, 187–202 (1983)
21. Fourie, A.B., Tshabalala, L.: Initiation of static liquefaction and the role of K0 consolidation. *Can. Geotech. J.* **42**(3), 892–906 (2005)
22. Wanatowski, D., Chu, J.: Static liquefaction of sand in plane strain. *Can. Geotech. J.* **44**, 299–313 (2007)
23. Penumadu, D., Skandarajah, A., et al.: Strain-rate effects in pressuremeter testing using a cuboidal shear device: experiments and modeling. *Can. Geotech. J.* **35**, 27–42 (1998)
24. Finge, Z., Doanh, T., Dubujet, P.: Undrained anisotropy of Hostun RF loose sand: new experimental investigations. *Can. Geotech. J.* **43**, 1195–1212 (2006)
25. Oh, E.Y.N., Bolton, M.W., Balasubramaniam, A.S.: Undrained behavior of lime treated soft clays. In: *The Proceedings of the International Offshore and Polar Engineering Conference*, vol. 18(2), pp. 607–612 (2008)
26. Niemunis, A., Grandas-Tavera, C.E., Prada-Sarmiento, L.F.: Anisotropic visco-hypoplasticity. *Acta Geotech.* **4**(4), 293–314 (2009)
27. Mašin, D.: Asymptotic behavior of granular materials. *Granul. Matter* **14**, 759–774 (2012)
28. Verdugo, R., Ishihara, K.: The steady state of sandy soils. *Soils Found.* **36**(2), 81–91 (1996)
29. Liu, M.F., Yao, Y.P., Kong, D.Q.: The experimental study of saturated structural K0-consolidated loess. *J. Xi'an Univ. Archit. Technol.* **40**(2), 238–242 (2008). (Natural Science Edition)